Mono- and dinuclear copper complexes coordinated on NNO-tridentate Schiff-base derivatives for copolymerization of cyclohexene oxide and cyclic anhydrides

Fu-Yin Cheng,[a] Chen-Yen Tsai,*[b] Kuan-Yeh Lu,[a] Chu-Chieh Lin*[a] and Bao-Tsan Ko*[a]

[a] Department of Chemistry, National Chung Hsing University, Taichung 402, Taiwan

[b] Department of Chemistry, Chinese Culture University, Taipei 111, Taiwan

* Corresponding author. E-mail: cyz21@ulive.pccu.edu.tw (C.-Y. Tsai); Tel: 886-2-28610511-25314; cchlin@mail.nchu.edu.tw (C.-C. Lin); Tel: 886-4-22840411-718; Fax: 886-4-22862547 and E-mail: btko@dragon.nchu.edu.tw (B.-T. Ko); Tel: 886-4-22840411-715; Fax: 886-4-22862547

Figure S1. UV–Vis spectra of complexes **1**–**10** in CH_2Cl_2 at 25 °C (a) $[M]_0 = 20\mu M$, (b) $[M]_0 = 1mM$.

Table S1. UV–Vis spectra of complexes **1**–**10** in CH_2Cl_2 at 25 °C.

Figure S2. EPR spectra of complexes **2**.

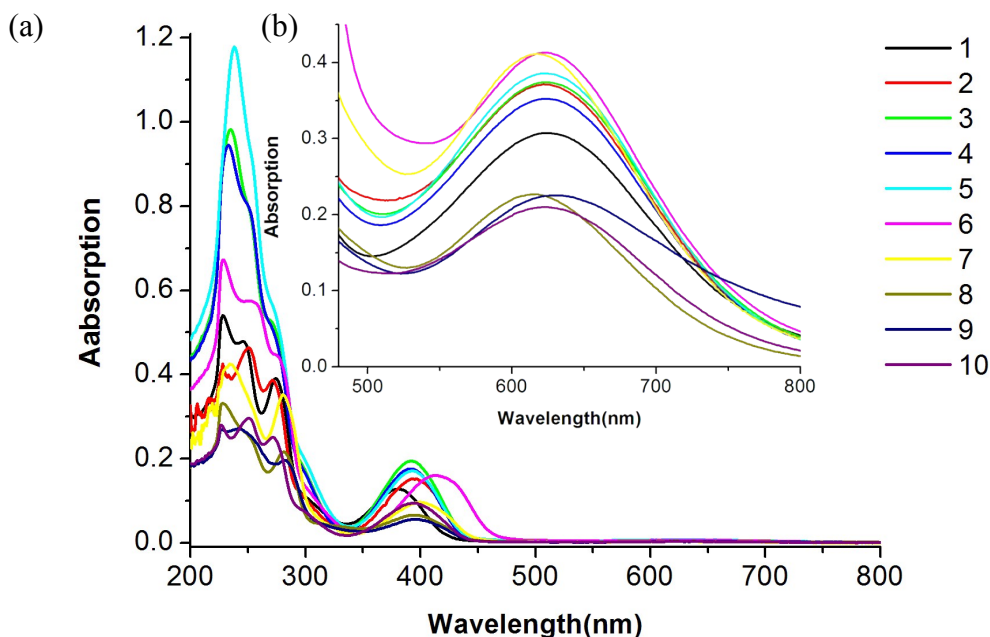**Table S2.** EPR spectra of complexes **1**–**10** at 25 °C.

Figure S3. ORTEP drawing of complex **3** with probability ellipsoids drawn at 50% level.

Figure S4. ORTEP drawing of complex **4** with probability ellipsoids drawn at 50% level.

Figure S5. ORTEP drawing of complex **6** with probability ellipsoids drawn at 50% level.

**Figure S6.** ORTEP drawing of complex **7** with probability ellipsoids drawn at 50% level.

Figure S7. ORTEP drawing of complex **8** with probability ellipsoids drawn at 50% level.

Figure S1. UV–Vis spectra of complexes **1**–**10** in CH_2Cl_2 at 25 °C (a) $[M]_0 = 20\mu M$, (b) $[M]_0 = 1mM$.

Table S1. UV–Vis spectra of complexes 1–10 in CH_2Cl_2 at 25 °C.

Complex	λmax,abs,(nm)(ε/10^4 $M^{-1}cm^{-1}$)	d-d, (nm) (ε/$M^{-1}cm^{-1}$)
(**1**):[(L^1)$_2$Cu$_2$(OAc)$_2$]	228(2.70) 246(2.39) 274(1.96) 381(0.64)	623(307.4)
(**2**):[(L^2)$_2$Cu$_2$(OAc)$_2$]	228(2.12) 251(2.32) 271(1.93) 394(0.76)	622(371.6)
(**3**):[(L^3)$_2$Cu$_2$(OAc)$_2$]	235(4.91) 252(3.91) 270(2.64) 392(0.97)	623(374.1)
(**4**):[(L^4)$_2$Cu$_2$(OAc)$_2$]	233(4.72) 251(3.98) 272(2.51) 391(0.88)	623(352.4)
(**5**):[(L^5)$_2$Cu$_2$(OAc)$_2$]	238(5.89) 253(4.60) 274(2.71) 393(0.85)	623(385.8)
(**6**):[(L^6)$_2$Cu$_2$(OAc)$_2$]	228(3.36) 251(2.88) 273(2.24) 412(0.80)	623(413.0)
(**7**):[(L^7)$_2$Cu$_2$(OAc)$_2$]	234(2.13) 255(1.57) 280(1.76) 400(0.49)	617(411.6)
(**8**):[(L^8)Cu(OAc)]	228(1.66) 249(1.29) 281(1.08) 396(0.33)	615(227.0)
(**9**):[(L^9)Cu(OAc)]	227(1.34) 241(1.35) 281(0.98) 396(0.28)	631(225.6)
(**10**):[(L^2)Cu(OAc)(H_2O)]	227(1.40) 251(2.98) 271(1.25) 395(0.47)	621(210.1)
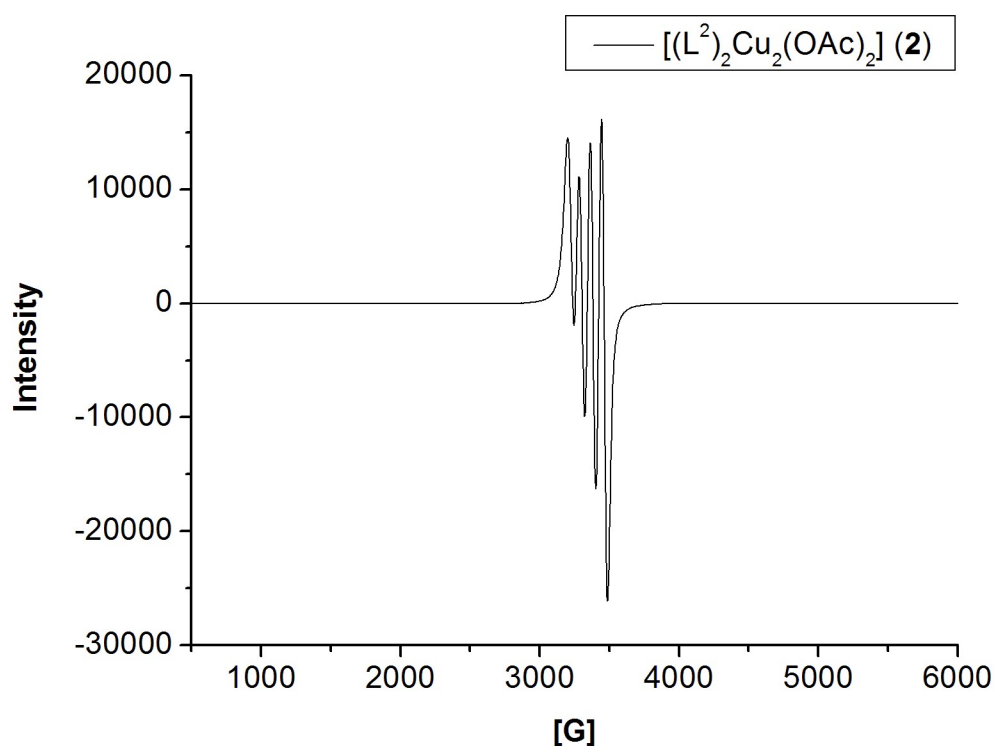
Figure S2. EPR spectra of complexes **2**.

Table S2. EPR spectra of complexes **1–10** at 25 ^{0}C.

Complex	g-factor	magnetic (μ)[a]
(1):[(L^1)$_2$Cu$_2$(OAc)$_2$]	2.0382	1.7651
(2):[(L^2)$_2$Cu$_2$(OAc)$_2$]	2.0370	1.7641
(3):[(L^3)$_2$Cu$_2$(OAc)$_2$]	2.0379	1.7649
(4):[(L^4)$_2$Cu$_2$(OAc)$_2$]	2.0375	1.7645
(5):[(L^5)$_2$Cu$_2$(OAc)$_2$]	2.0386	1.7654
(6):[(L^6)$_2$Cu$_2$(OAc)$_2$]	2.0389	1.7657
(7):[(L^7)$_2$Cu$_2$(OAc)$_2$]	2.0275	1.7556
(8):[(L^8)Cu(OAc)]	2.0345	1.7619
(9):[(L^9)Cu(OAc)]	2.0372	1.7643

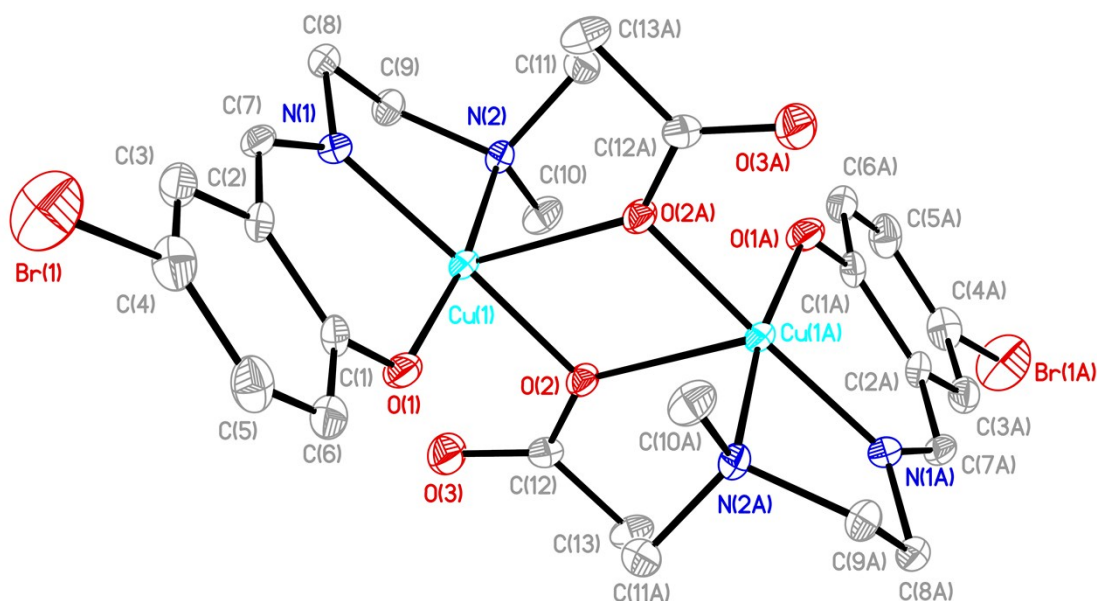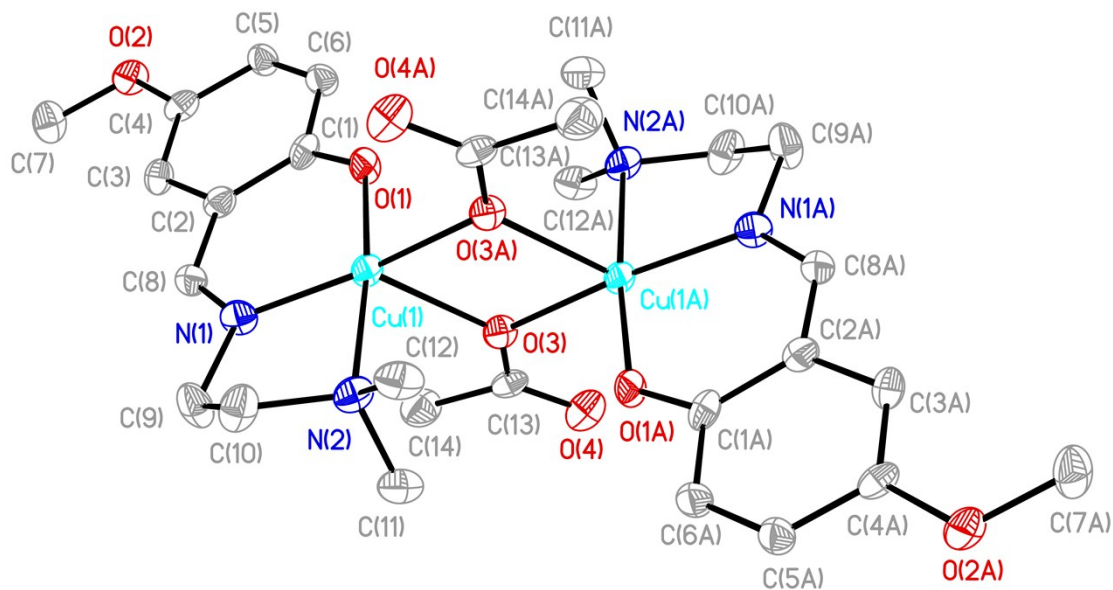| (**10**):[(L²)Cu(OAc)(H₂O)]	2.0382	1.7651
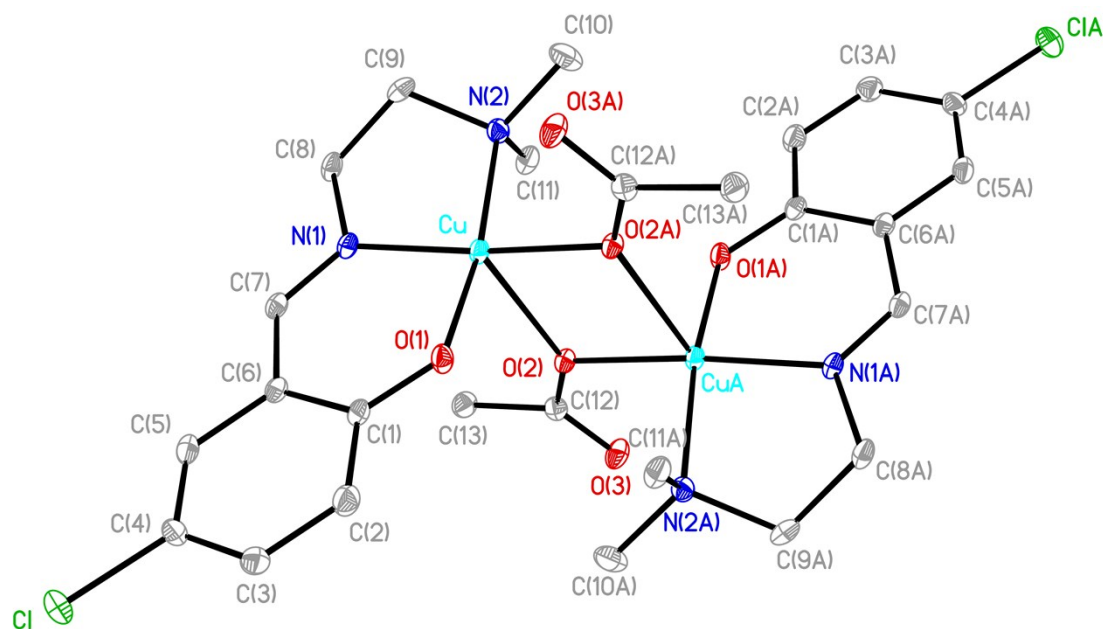
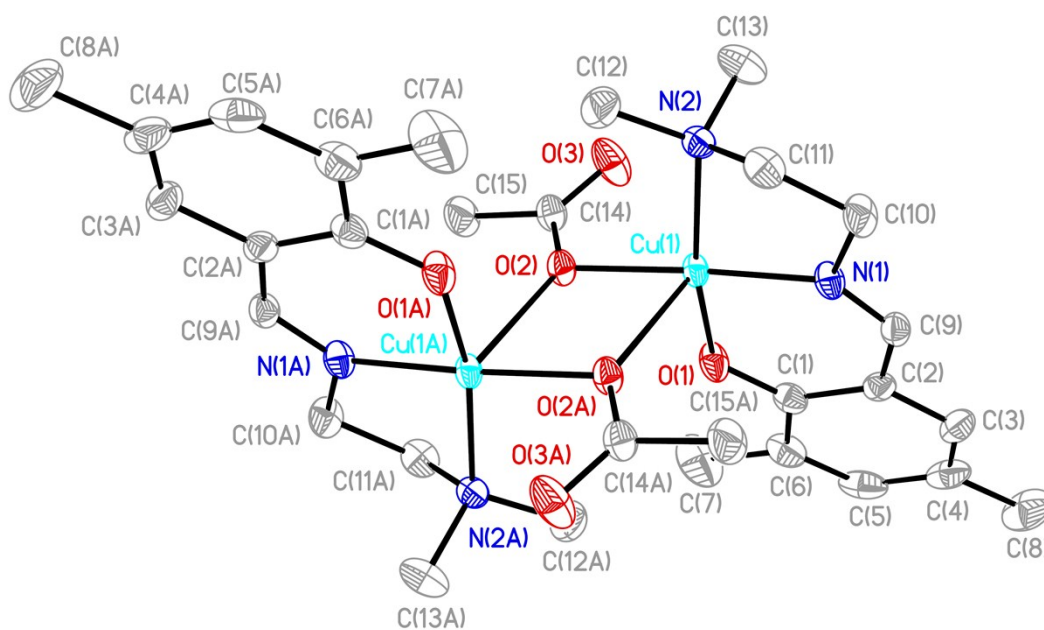**Figure S3.** ORTEP drawing of complex **3** with probability ellipsoids drawn at 50% level. Hydrogen atoms are omitted for clarity. Selected bond lengths (Å) and angles (deg): Cu-O(1) 1.937(2), Cu-N(1) 1.953(2), Cu-O(2)A 1.9603(17), Cu-N(2) 2.105(2), Cu-O(2) 2.3468(18), O(1)-Cu-N(1) 91.12(9), O(1)-Cu-O(2)A 89.17(8), N(1)-Cu-O(2)A 173.64(8), O(1)-Cu-N(2) 170.78(8), N(1)-Cu-N(2) 83.45(9), O(2)A-Cu-N(2) 95.41(8), O(1)-Cu-O(2) 89.30(7), N(1)-Cu-O(2) 109.05(8), O(2)A-Cu-O(2) 77.30(8), N(2)-Cu-O(2) 99.50(8).
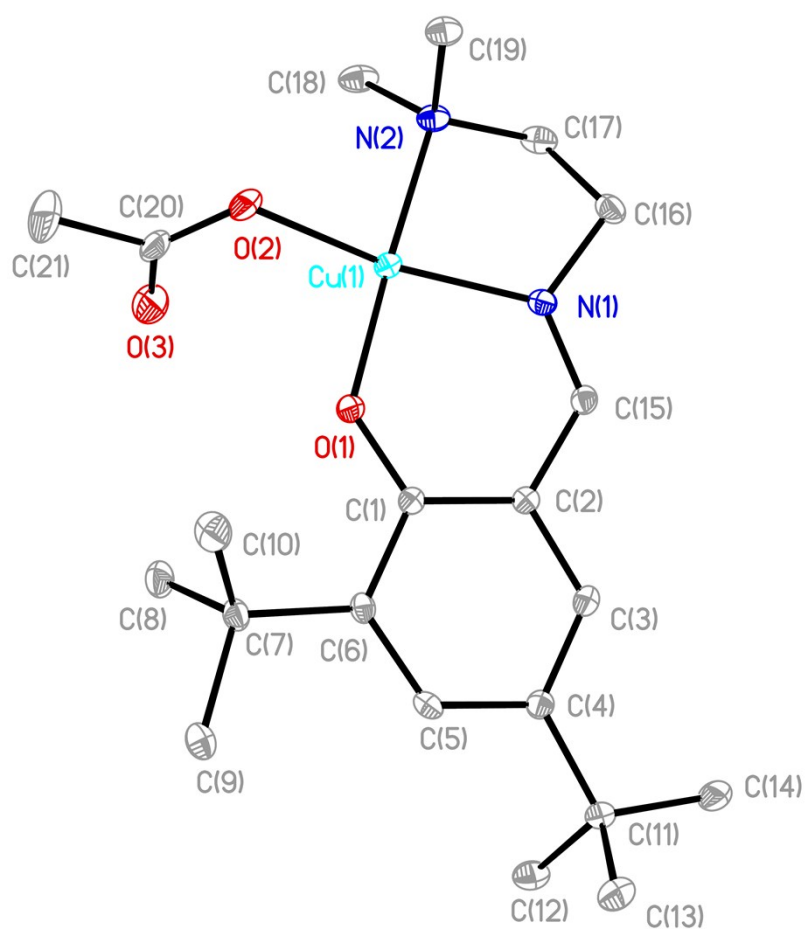
Figure S4. ORTEP drawing of complex **4** with probability ellipsoids drawn at 50% level. Hydrogen atoms are omitted for clarity. Selected bond lengths (Å) and angles (deg): Cu(1)-O(1) 1.9435(17), Cu(1)-O(2) 1.9574(17), Cu(1)-N(1) 1.961(2), Cu(1)-N(2) 2.097(2),   Cu(1)-O(2)A 2.4073(16), O(1)-Cu(1)-O(2) 90.99(7), O(1)-Cu(1)-N(1) 91.04(8), O(2)-Cu(1)-N(1) 174.90(8), O(1)-Cu(1)-N(2) 171.57(7), O(2)-Cu(1)-N(2) 94.71(7), N(1)-Cu(1)-N(2) 82.78(8), O(1)-Cu(1)-O(2)A 88.93(7), O(2)-Cu(1)-O(2)A 74.71(7), N(1)-Cu(1)-O(2)A 110.00(7),   N(2)-Cu(1)-O(2)A 98.56(7).

Figure S5. ORTEP drawing of complex **6** with probability ellipsoids drawn at 50% level. Hydrogen atoms are omitted for clarity. Selected bond lengths (Å) and angles (deg): Cu(1)-O(1) 1.924(3), Cu(1)-O(3)A 1.963(3), Cu(1)-N(1) 1.962(4), Cu(1)-N(2) 2.114(4), Cu(1)-O(3) 2.354(3), O(1)-Cu(1)-O(3)A 90.75(13), O(1)-Cu(1)-N(1) 91.69(13), O(3)A-Cu(1)-N(1) 170.32(13), O(1)-Cu(1)-N(2) 174.31(13), O(3)A-Cu(1)-N(2) 94.19(14), N(1)-Cu(1)-N(2) 82.97(14), O(1)-Cu(1)-O(3) 87.66(12), O(3)A-Cu(1)-O(3) 74.36(13), N(1)-Cu(1)-O(3) 115.10(14), N(2)-Cu(1)-O(3) 96.38(13).

Figure S6. ORTEP drawing of complex **7** with probability ellipsoids drawn at 50% level. Hydrogen atoms are omitted for clarity. Selected bond lengths (Å) and angles (deg): Cu(1)-O(1) 1.9193(15), Cu(1)-N(1) 1.9467(18), Cu(1)-O(2), 1.9636(14), Cu(1)-N(2) 2.0762(17), O(1)-Cu(1)-N(1) 91.97(7), O(1)-Cu(1)-O(2) 88.94(6), N(1)-Cu(1)-O(2) 174.91(6), O(1)-Cu(1)-N(2) 164.52(7), N(1)-Cu(1)-N(2) 82.60(7), O(2)-Cu(1)-N(2) 97.75(7).

Figure S7. ORTEP drawing of complex **8** with probability ellipsoids drawn at 50% level. Hydrogen atoms are omitted for clarity. Selected bond lengths (Å) and angles (deg): Cu(1)-O(1) 1.903(2), Cu(1)-N(1) 1.928(3), Cu(1)-O(2) 1.951(3), Cu(1)-N(2) 2.051(3), O(1)-Cu(1)-N(1) 92.48(11), O(1)-Cu(1)-O(2) 89.10(11), N(1)-Cu(1)-O(2) 161.03(11), O(1)-Cu(1)-N(2) 177.62(11), N(1)-Cu(1)-N(2) 85.22(12), O(2)-Cu(1)-N(2) 92.86(12).